Toxicology Letters 229 (2014) 178–189

Contents lists available at ScienceDirect

Toxicology Letters

journal homepage: www.elsevier.com/locate/toxlet

Piperazine designer drugs induce toxicity in cardiomyoblast h9c2 cells through mitochondrial impairment

Marcelo Dutra Arbo [a,*], Renata Silva [a], Daniel José Barbosa [a], Diana Dias da Silva [a], Luciana Grazziotin Rossato [a,b], Maria de Lourdes Bastos [a], Helena Carmo [a]

[a] REQUIMTE, Laboratório de Toxicologia, Departamento de Ciências Biológicas, Faculdade de Farmácia, Universidade do Porto, Rua Jorge Viterbo Ferreira 228, Porto 4050-313, Portugal
[b] Instituto de Ciências Biológicas, Curso de Farmácia, Universidade de Passo Fundo (UPF) Campus I, km 292, BR 285, Passo Fundo, Rio Grande do Sul 99052-900, Brazil

HIGHLIGHTS

- Piperazine derivatives presented cytotoxicity, being TFMPP the most cytotoxic.
- Piperazine designer drugs significantly increased Ca^{2+} intracellular levels.
- All drugs caused decreased intracellular ATP and mitochondrial membrane potential.
- Mitochondrial permeability transition pore seems to play a role in cytoxicity.
- There were found early apoptotic cells and cells undergoing secondary necrosis.

ARTICLE INFO

Article history:
Received 14 April 2014
Received in revised form 18 June 2014
Accepted 20 June 2014
Available online 23 June 2014

Keywords:
Piperazine designer drugs
Mitochondrial impairment
Ca^{2+} overload
Mitochondrial membrane potential
Apoptosis
Mitochondrial permeability transition pore

ABSTRACT

Abuse of synthetic drugs is widespread among young people worldwide. In this context, piperazine derived drugs recently appeared in the recreational drug market. Clinical studies and case-reports describe sympathomimetic effects including hypertension, tachycardia, and increased heart rate. Our aim was to investigate the cytotoxicity of *N*-benzylpiperazine (BZP), 1-(3-trifluoromethylphenyl) piperazine (TFMPP), 1-(4-methoxyphenyl) piperazine (MeOPP), and 1-(3,4-methylenedioxybenzyl) piperazine (MDBP) in the H9c2 rat cardiac cell line. Complete cytotoxicity curves were obtained at a 0–20 mM concentration range after 24 h incubations with each drug. The EC_{50} values (μM) were 343.9, 59.6, 570.1, and 702.5 for BZP, TFMPP, MeOPP, and MDBP, respectively. There was no change in oxidative stress markers. However, a decrease in total GSH content was noted for MDBP, probably due to metabolic conjugation reactions. All drugs caused significant decreases in intracellular ATP, accompanied by increased intracellular calcium levels and a decrease in mitochondrial membrane potential that seems to involve the mitochondrial permeability transition pore. The cell death mode revealed early apoptotic cells and high number of cells undergoing secondary necrosis. Among the tested drugs, TFMPP seems to be the most potent cytotoxic compound. Overall, piperazine designer drugs are potentially cardiotoxic and support concerns on risks associated with the intake of these drugs.

1. Introduction

Piperazine designer drugs emerged in the drug market for recreational purposes in the early 2000s. They can be divided into two classes, the benzylpiperazines such as *N*-benzylpiperazine (BZP) and its methylenedioxy-analogue 1-(3,4-methylenedioxybenzyl) piperazine (MDBP), and the phenylpiperazines such as 1-(3-chlorophenyl) piperazine (*m* CPP), 1-(4-fluorophenyl) piperazine (*p* FPP), 1-(3-trifluoromethylphenyl) piperazine (TFMPP), and 1-(4-methoxyphenyl) piperazine (MeOPP) (Fig. 1). Generally, they are consumed as capsules, tablets or pills but also in powder or liquid forms (Gee et al., 2005) under

* Corresponding author. Tel.: +351 220428597.
E-mail addresses: m.arbo@terra.com.br, marcelo.arbo@gmail.com (M.D. Arbo).

http://dx.doi.org/10.1016/j.toxlet.2014.06.031
0378-4274/

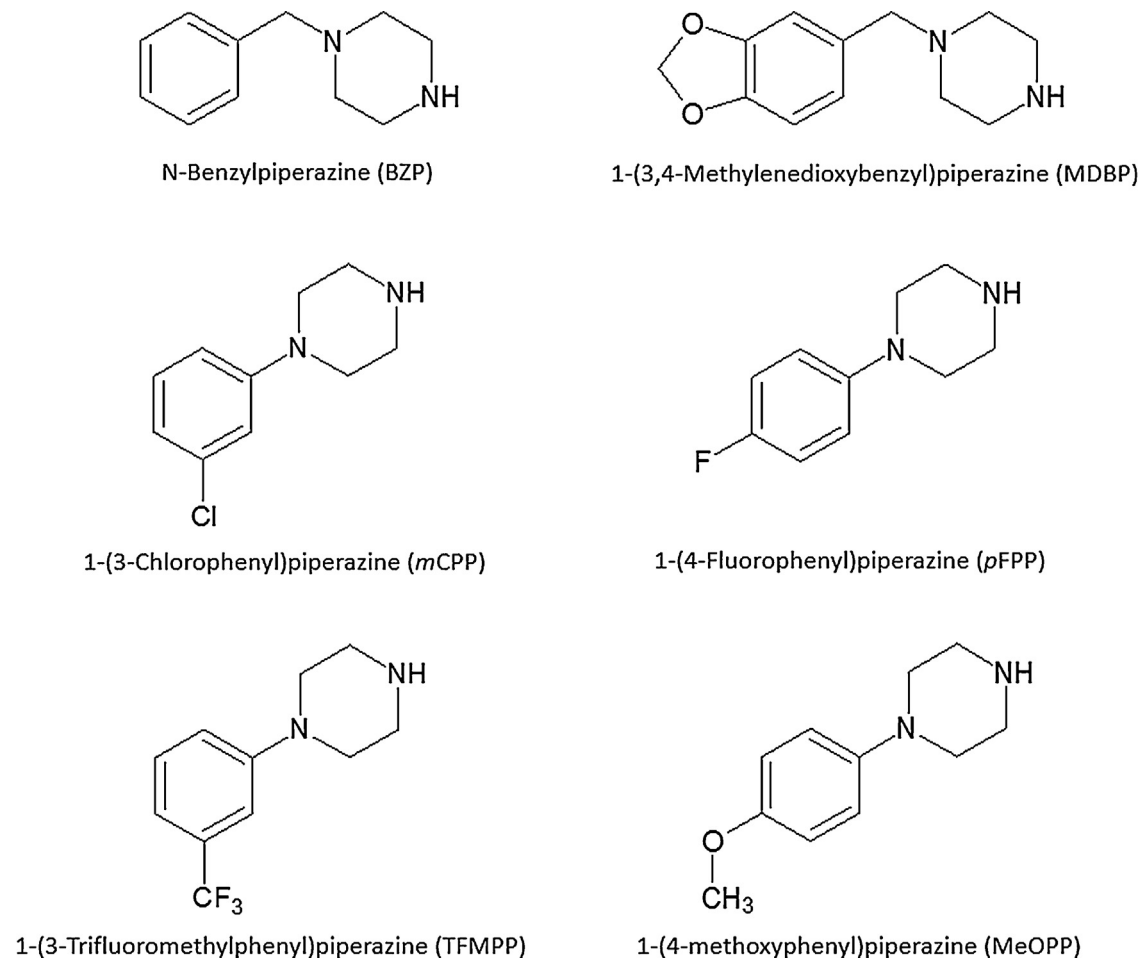

Fig. 1. Chemical structure of some piperazine designer drugs.

several names, such as "Rapture," "Frenzy," "Bliss," "Charge," "Herbal ecstasy," "A2," "Legal X," "Legal E," or simply party pills. They can also appear as adulterants of MDMA and cocaine (Staack et al., 2007).

In humans, piperazines are readily absorbed from the gastrointestinal tract (Antia et al., 2009; Schep et al., 2011). The information available on blood concentrations and pharmacokinetic distribution data is extremely limited. Blood concentrations measured at clinical studies with human volunteers reached approximately 1 μM after 200 mg of orally administrated BZP (Antia et al., 2009) and 0.1 μM after 60 mg of TFMPP (Antia et al., 2010). However, higher (up to 25 times) and largely discrepant blood concentrations were reported after intoxication with BZP and TFMPP (Gee et al., 2008; Kovaleva et al., 2008; Wood et al., 2008; Antia et al., 2009, 2010; Gee et al., 2010). Moreover, it is known that piperazine designer drugs readily cross the blood–brain barrier and interestingly, animal studies have shown that the TFMPP C_{max} brain-to-blood concentration ratio was in excess of one order of magnitude (Schep et al., 2011) indicating that these drugs achieve high tissue concentrations. The piperazine designer drugs are mainly metabolized in the liver, being the phenylpiperazines more extensively metabolized than the benzylpiperazines, and excreted almost exclusively as metabolites (Maurer et al., 2004). The main metabolic pathways that were already described for the piperazine designer drugs in animals and in humans are the aromatic hydroxylation of BZP (Staack and Maurer, 2005), TFMPP (Staack et al., 2003), and MeOPP (Staack et al., 2004), and the demethylenation of MDBP (Staack and Maurer, 2004). The rates of urinary excretion of the drugs and metabolites seem to vary widely among individuals (Austin and Monasterio, 2004).

Phenylpiperazine designer drugs, such as TFMPP, are non-selective 5-HT agonists, and also act as substrates for serotonin transporters (SERTs). On the other hand, benzylpiperazine derivatives, namely BZP, act on central dopaminergic substrates such as D_1-like receptors and dopamine transporters (DATs). It has been reported that the combined use of BZP and TFMPP in pills (mixed at a 2:1 ratio, in most cases) mimics the effects of 3,4-methylenedioxymethamphetamine (MDMA, ecstasy) in humans. It is, therefore, believed that this combination aggregates the stimulant effect of BZP, through its dopaminergic action, with the hallucinogenic effects of TFMPP, via serotonergic activation (for review see Arbo et al., 2012).

Accordingly, cardiovascular effects dependent on both dopaminergic and serotonergic stimulation were noted after the intake of piperazine designer drugs, and a predominance of adrenergic effects in the peripheral system, characteristic of a sympathomimetic toxindrome, was observed (Schep et al., 2011). Most common effects include *d*-amphetamine-like effects (Lin et al., 2011), tachycardia, hypertension, anxiety, vomiting, headache, migraine, palpitations, confusion, collapse, and seizure (Gijsman et al., 1998; Gee et al., 2005; Feuchtl et al., 2004; Thompson et al., 2010). In a randomized, double-blind, placebo-controlled study, a single administration of 200 mg BZP to women induced an increase in systolic and diastolic blood pressure and heart rate comparing to placebo (Lin et al., 2009). The same cardiovascular effects were found in other studies using a single administration of a BZP/

TFMPP combination (Thompson et al., 2010; Lin et al., 2011). Wood et al. (2008) reported a case of three male young adults presenting dissociative symptoms, agitation with bruxism, nausea, and features of sympathomimetic toxicity, with dilated pupils and tachycardia after the intake of four tablets of a drug thought to be ecstasy but contaning BZP and TFMPP. In New Zealand, two cases involving an adult woman and a young man were reported, in which the patients developed status epilepticus, hyperthermia, tachycardia, and tachypnea after BZP intake (Gee et al., 2010). In a non-fatal case of mCPP overdose, a female patient developed anxiety, agitation, drowsiness, flushing, visual disturbances, and tachycardia (Kovaleva et al., 2008).

The cardiovascular effects of recreational drugs are, to some extent, predictable because the receptors and transporters on which they act are located both in the central nervous system and in the periphery. Drugs acting on serotonergic, dopaminergic, or noradrenergic systems are, therefore, likely to induce vasoconstriction and/or tachycardia and arrhythmia. Extreme activation of the sympathetic control of the cardiovascular system can lead to profound vasoconstriction and ischemia. The resultant hypertension is a risk factor for strokes and myocardial infarcts, which are more common in chronic sympathomimetic drug abusers. The cardiac effect of sympathetic stimulation produces both ischemia (coronary vasoconstriction) and an increased oxygen demand (as a consequence of increased myocardial contractility). Sympathomimetic drugs also induce arrhythmias, which probably contribute to fatalities (Dawson and Moffatt, 2012).

Besides the activation of central and peripheral neurotransmission, these drugs may act directly at the cardiomyocyte level to produce cytotoxicity. This has been noted for example with the cardiotoxicity mechanisms of amphetamines, such as MDMA, that seem to involve mitochondrial impairment and metabolic bioactivation of the drugs and intracellular Ca^{2+} homeostasis, which can, in turn, abnormally alter myocardial excitability and contractility (Tiangco et al., 2005; Carvalho et al., 2012).

Notwithstanding, in the corresponding drug scene, piperazines have the reputation of being safe, and there are presently no studies regarding their toxicity at the cellular level that could help understanding the aforementioned detrimental effects of these drugs. The aim of this work was to study the in vitro cardiotoxicity of the piperazine designer drugs BZP, TFMPP, MeOPP, and MDBP using the H9c2 cardiac cell line. The H9c2 is a cell line derived from rat heart (Kimes and Brandt, 1976), that is considered a valuable model to assess in vitro cardiotoxicity, especially because these cells biochemical and electrophysiological properties are comparable to those of adult cardiomyocytes and adequately mimic the metabolic capacity of the rat heart (Zordoky and El-Kadi, 2007).

2. Material and methods

2.1. Chemicals

N-Benzylpiperazine (BZP, 99.3% purity) was purchased from Chemos GmbH (Regenstauf, Germany), 1-(3-trifluoromethylphenyl) piperazine (TFMPP, 98% purity) was acquired from Alfa Aesar (Karlsruhe, Germany), 1-(4-methoxyphenyl) piperazine (MeOPP, 96% purity) was purchased from Acros Organics (New Jersey, USA), and 1-(3,4-methylenedioxybenzyl) piperazine (MDBP, 97% purity) was purchased from Aldrich Chemistry (Steinheim, Germany). Fetal bovine serum (FBS), trypsin (0.25%)–EDTA (1 mM), and antibiotic (10,000 U/mL penicillin, 10,000 μg/mL streptomycin), Hanks balanced salt solution (HBSS), and phosphate buffer (PBS) were obtained from Gibco Laboratories (Lenexa, KS, USA). Dulbecco's modified eagle's medium (DMEM) with 4500 mg/L glucose, dichlorodihydrofluorescein diacetate (DCFH-DA), tetramethylrhodamine ethyl ester perchlorate (TMRE), reduced glutathione (GSH), oxidized glutathione (GSSG), glutathione reductase (GR, EC 1.6.4.2), 2-vinylpyridine, reduced β-nicotinamide adenine dinucleotide (β-NADH), 3-(4,5-dimethylthiazol-2-yl)-2,5-diphenyltetrazolium bromide (MTT), 5,5-dithio-bis(2-nitrobenzoic) acid (DTNB), *N*-acetyl-Asp-Glu-Val-Asp-*p*-nitroaniline (Ac-DEVD-pNA), 4-(2-hydroxyethyl) piperazine-1-ethanesulfonic acid (HEPES), 3-[(3-cholamidopropyl) dimethylammonio]-1-propanesulfonate hydrate (CHAPS), dithiothreitol (DTT), ethylenediaminetetraacetic acid (EDTA), luciferin, luciferase, campthotecin, and cyclosporine A were obtained from Sigma–Aldrich (St. Louis, USA). Fluo-3 AM was obtained from Molecular Probes (Eugene, OR). Dimethylsulfoxide (DMSO), perchloric acid ($HClO_4$), sodium phosphate dibasic (Na_2HPO_4), sodium phosphate monobasic (NaH_2PO_4), potassium bicarbonate ($KHCO_3$), hydrogen peroxide (H_2O_2), sodium chloride (NaCl), and glycerol were obtained from Merck (Darmstadt, Germany). Flow cytometry reagents (BD Facs-Flow™ and Facs-Clean™) were purchased from BD (Becton, Dickinson and Company, San Jose, CA, USA).

2.2. H9c2 cell culture

The H9c2 cell line was a generous gift from Dr. Vilma Sardão, Center for Neurosciences and Cellular Biology, University of Coimbra, Portugal. The cells were cultured in DMEM supplemented with 10% FBS, 100 U/mL of penicillin, and 100 μg/mL of streptomycin in 75 cm^2 tissue culture flasks at 37 °C in a humidified 5% CO_2–95% air atmosphere. The cells were fed every 2–3 days, and sub-cultured once 70–80% confluence was reached.

2.3. Cytotoxicity assay

For the evaluation of cytotoxicity, the MTT reduction assay was performed as previously described (Rossato et al., 2013). This assay measures dehydrogenase activity, an indicator of metabolically active mitochondria, and therefore, of cell viability. Cells were seeded at a density of 35,000 cells/mL in 48-well plates (final volume of 250 μL; ~8000 cells/cm^2). Stock solutions of BZP were made up in PBS. Stock solutions of TFMPP, MeOPP, and MDBP were made in DMSO. In these cases, 0.1% DMSO in culture medium was used as negative control. All stock solutions were stored at −20 °C and freshly diluted on the day of the experiment. Concentration–response curves were obtained incubating the cells with 0–20 mM of BZP, TFMPP, MeOPP, or MDBP for 24 h at 37 °C. Triton X-100 1% was used as positive control. After the incubation period, the medium was removed and replaced with fresh medium containing 0.5 mg/L MTT. The cells were incubated at 37 °C for 4 h. After incubation, the cell culture medium was removed, and the formed formazan crystals dissolved in DMSO. The absorbance was measured at 550 nm in a multi-well plate reader (BioTek Instruments, Vermont, USA). To reduce inter-experimental variability, data were normalized and scaled between 0% (negative controls) and 100% effect (positive controls). Results were graphically presented as percentage of cell death vs concentration (μM). All drugs were tested in three independent experiments with each concentration tested in six replicates within each experiment.

2.4. Neutral red (NR) uptake assay

To confirm the results obtained with the MTT reduction assay, we performed the NR uptake assay. This assay is based on the ability of viable cells to incorporate and bind the weak cationic dye NR, which penetrates into the cells by non-ionic diffusion, accumulating in lysosomes by interaction with anionic sites in the lysosomal matrix (Labonne et al., 2009). At the end of 24 h incubations of H9c2 cells with 0–20 mM of BZP, TFMPP, MeOPP, or

MDBP, the medium was replaced by new medium containing 50 μg/mL NR. The cells were incubated at 37 °C in a humidified, 5% CO_2–95% air atmosphere for 3 h allowing the lysosomes of viable cells to take up the dye. Thereafter, the cells were carefully washed with 200 μL of HBSS to eliminate extracellular dye and lysed with a 50% ethanol–1% glacial acid acetic solution. Triton X-100 1% was used as positive control. The absorbance was measured at 540 nm in a multi-well plate reader (BioTek Instruments, Vermont, USA). The percent cell death relative to that of the control cells was used as the cytotoxicity measure.

2.5. Intracellular ROS and RNS production

The intracellular reactive oxygen (ROS) and nitrogen (RNS) species production was monitored by means of the DCFH-DA assay as previously described (Dias da Silva et al., 2013b). The sensitive DCFH-DA lipophilic probe readily penetrates the cells producing 2′,7′-dichlorodihydrofluorescein (DCFH) after hydrolysis, which further reacts with intracellular ROS and RNS, including the hydroxyl radical and hydrogen peroxide, generating green fluorescent 2′,7′-dichlorofluorescein (DCF), which is polar and trapped within the cells (Rao et al., 1992; Smith and Weidemann, 1993). For this determination, cells were seeded at a density of 35,000 cells/mL in 48-well plates (final volume of 250 μL, ~8000 cells/cm^2) and allowed to grow for 48 h. On the day of the experiment, the cells were pre-incubated with 10 μM DCFH-DA for 30 min, at 37 °C, in the dark. As DCFH-DA is a non-water-soluble powder, it was initially prepared as a 4 mM stock solution in DMSO and made up to the final concentration in fresh culture medium (ensuring that the final concentration of DMSO did not exceed 0.05%) immediately before each experiment. The cells were then rinsed with HBSS and incubated with the piperazine designer drugs (1000 and 2000 μM BZP, MeOPP, or MDBP or 50 and 500 μM for TFMPP) at 37 °C. H_2O_2 (150 μM) was used as a positive control. Fluorescence was recorded on a fluorescence microplate reader (BioTek Instruments, Vermont, USA) set to 485 nm excitation and 530 nm emission at times 0, 1, 2, 3, 4, 5, 6, 7, 8, and 24 h after incubation. The data obtained were normalized to negative controls on a plate-by-plate basis and calculated as fold increase over control conditions from three independent experiments with each concentration tested in three replicates within each experiment.

2.6. Measurement of intracellular total glutathione (tGSH), GSH, and GSSG levels

Cells were seeded at a density of 35,000 cells/mL in 55 cm^2 Petri dishes (final volume of 12.5 mL, ~8000 cell/cm^2) and grown for 48 h. The medium was then replaced and cells were incubated at 37 °C with the piperazine designer drugs (1000 and 2000 μM BZP, MeOPP, or MDBP or 50 and 500 μM for TFMPP). After a 24 h incubation period, the medium was removed, and the cells were kept on ice while being scraped in PBS, pH 7.4. After centrifugation (210 × *g*, 5 min, 4 °C), the supernatant was removed. The pellet of cells was lysed with 5% $HClO_4$ and centrifuged (16,000 × *g*, 10 min, 4 °C). The obtained supernatant was frozen at −20 °C until further determination of tGSH and GSSG levels, evaluated by the DTNB–GSSG reductase recycling assay, as previously described (Rossato et al., 2013). Briefly, the acidic supernatant was neutralized with an equal volume of 0.76 M $KHCO_3$ and centrifuged (16,000 × *g*, 2 min, 4 °C). Total glutathione was determined by transfering, in triplicate, 100 μL of the neutralized supernatants, standards or blank (5% $HClO_4$, w/v) to a 96-well plate, followed by the addition of 65 μL of freshly prepared reagent containing 0.24 mM NADPH and 0.7 mM DTNB in phosphate buffer (71.5 mM Na_2HPO_4, 71.5 mM NaH_2PO_4, and 0.63 mM EDTA; pH 7.5). The plates were then incubated for 15 min, at 30 °C, in a microplate reader (BioTek Instruments, Vermont, USA), prior to the addition of 40 μL per well of a freshly prepared 10 U/mL glutathione reductase solution in phosphate buffer. The stoichiometric formation of 5-thio-2-nitrobenzoic acid (TNB) was followed every 10 s for 3 min at 415 nm at 30 °C, and compared with a standard curve performed for all readings. For the determination of GSSG, 10 μL of 2-vinylpyridine was added to 200 μL aliquots of the acidic supernatants and mixed continuously for 1 h at 0 °C for derivatization of the sulfhydryl groups (SH). GSSG was then measured as described for tGSH. The GSH content was calculated by subtracting the GSSG from the tGSH values [GSH = tGSH − (2 × GSSG)]. The final results were expressed as percentage of control conditions from five independent experiments with each concentration tested in three replicates within each experiment.

2.7. Influence of piperazine designer drugs on glutathione reductase (GR) activity

The activity of GR was evaluated by following the oxidation of NADPH consumed during the reduction of GSSG at 340 nm, at a constant temperature of 30 °C (Remião et al., 2000). The enzyme activity was determined by transferring 170 μL of a reaction mixture containing 1 mM GSSG, 71.5 mM Na_2HPO_4, 71.5 mM NaH_2PO_4, and 0.63 mM EDTA; pH 7.5, to which 50 μL of a freshly prepared 0.5 U/mL glutathione reductase solution in phosphate buffer and 100, 500, 1000, and 2000 μM BZP, MeOPP, or MDBP or 5, 50, 100, and 500 μM TFMPP were added. After 2 min pre-incubation, the reaction was initiated by the addition of 30 μL 1 mM NAPH in phosphate buffer. The kinectics of the reaction was monitored for 5 min at 20 s intervals. A blank assay containing all components of the reaction mixture except the enzyme was performed to evaluate the non-enzymatic oxidation of NADPH, which was subtracted from the assay values. As a positive control, DHBA (3,4-dihydroxybenzylamine) was used. The final results were expressed as percentage of control conditions from three independent experiments with each concentration tested in three replicates within each experiment.

2.8. Measurement of intracellular ATP levels

Cells were seeded, treated and incubated following the same protocol used for the measurement of glutathione levels. After centrifugation (210 × *g*, 5 min, 4 °C), the supernatant was removed. The pellet of cells was lysed with 5% $HClO_4$, centrifuged (16,000 × *g*, 10 min, 4 °C), and the supernatant obtained was frozen at −20 °C until further determination of the ATP intracellular content. The ATP levels were quantified by a bioluminescence assay, as described by Rossato et al. (2013). Briefly, the acidic supernatant was neutralized with an equal volume of 0.76 M $KHCO_3$ and centrifuged (16,000 × *g*, 1 min, 4 °C). The ATP contents were then measured in duplicate in 96-well white plates, by adding 100 μL of the neutralized supernatants, standards or blank (5% $HClO_4$, w/v) and 100 μL of the luciferin/luciferase solution [0.15 mM luciferin, 300,000 light units of luciferase from *Photinus pyralis* (American firefly), 50 mM glycine, 10 mM $MgSO_4$, 1 mM Tris, 0.55 mM EDTA, 1% BSA (pH 7.6)]. The emitted light intensity was determined using a luminescence microplate reader (BioTek Instruments, Vermont, USA) and compared with a standard curve performed within each experiment. The final results were expressed as percentage of control conditions from five independent experiments with each concentration tested in two replicates within each experiment.

2.9. Flow cytometry analysis of intracellular Ca^{2+} levels

Intracellular Ca^{2+} levels were evaluated with the sensitive fluorochrome Fluo3-AM. After uptake by live cells, Fluo3-AM is enzymatically hydrolyzed by intracellular esterases to Fluo3,

which binds Ca^{2+} and exhibits an increase in fluorescence intensity. A protocol previously described (Rossato et al., 2013) was used with minor modifications. Cells were seeded at a density of 35,000 cells/mL in six-well plates (final volume of 2.5 mL, ~9,000 cells/cm^2). After 48 h, the medium was replaced by fresh medium containing 500 and 1000 μM BZP or MDBP, or 250 and 500 μM MeOPP, or 10, 50, and 100 μM TFMPP. Twenty-four hours after exposure, the cells were harvested by trypsinization (0.05% trypsin/EDTA), centrifuged (300 × *g*, 5 min, 4 °C), and then loaded with 10 μM Fluo3-AM in 50 μL of heated serum-free DMEM without phenol red, for 30 min, at 37 °C, in a water bath with shaking. After this incubation period, the cells were centrifuged (300 × *g*, 5 min, 4 °C) washed by resuspending in 500 μL of heated HBSS (with Ca^{2+} and Mg^{2+}), centrifuged again (300 × *g*, 5 min, 4 °C), and kept on ice until flow cytometry analysis.

Sample analysis was performed in a FACSCalibur™ flow cytometer (BD, CA, USA), equipped with a 488 nm argon ion laser, using CellQuest software (BD Biosciences). The green fluorescence of Fluo3 was measured by a 530 ± 15 nm band-pass filter (FL1). After resuspending the cell pellet in HBSS (+/+) with 0.5 μg/mL propidium iodide (PI) (after permeating death cells, PI interlaces with the nucleic acid helix with consequent increase in fluorescence intensity emission at 615 nm), data from at least 15,000 viable cells (based on their forward and side light scatter) were collected from each test condition. In order to detect a possible contribution from cells auto-fluorescence to the analyzed fluorescence signals, portions of cell suspension (with or without exposure to the drugs), which were not incubated with Fluo3-AM, were analyzed in the 530 ± 15 nm band-pass filter (FL1). Results are presented as Fluo3 fluorescence intensity (percentage of control) from at least six independent experiments with each concentration tested in two replicates within each experiment.

2.10. Assesment of mitochondrial membrane potential ($\Delta\psi m$)

Assessment of mitochondrial integrity was performed by measuring TMRE inclusion as described by Dias da Silva et al. (2013c). TMRE is a cell permeable fluorescent dye that specifically stains live mitochondria, and accumulates in proportion to the mitochondrial membrane potential ($\Delta\psi m$) (Scaduto and Grotyohann, 1999). Cells were seeded at a density of 35,000 cells/mL in 48-well plates (final volume of 250 μL; ~8000 cells/cm^2). After 48 h, the medium was gently aspirated, and the cells were incubated with the piperazine designer drugs (500, 1000, and 2000 μM for BZP, MeOPP, or MDBP or 10, 50, 100, 500, and 1000 μM for TFMPP). At the end of the 24 h incubation period, the medium was replaced by fresh medium containing 2 μM TMRE, and incubated at 37 °C, for 30 min, in the dark. As TMRE is a non water-soluble powder, a 2 mM stock solution was initially prepared in DMSO and stored in the dark. Afterwards, the medium was gently aspirated and replaced by 0.2% BSA in HBSS. Fluorescence was measured on a fluorescence microplate reader (BioTek Instruments, Vermont, USA) set to 544 nm excitation and 590 nm emission. The data obtained were normalized on a plate-by-plate basis to the values of the respective controls and calculated as the percentage of control conditions from at least six independent experiments with each concentration tested in three replicates within each experiment. Although rhodamines can undergo self-quenching at high concentrations (up to 150 nM), the use of low concentrations may cause a loss of sensibility in detecting small $\Delta\psi m$ depolarizations. The 2 μM TMRE tested concentration has been successful in detecting $\Delta\psi m$ alterations in previous works (Dias da Silva et al., 2013c).

2.11. Inhibition of the mitochondrial permeability transition pore (MPTP)

The mitochondrial permeability transition pore is sensitive to cyclosporin A (CsA) that blocks the opening of this pore. To evaluate the role of MPTP in the cytotoxicity mediated by piperazine designer drugs, H9c2 cells were seeded at a density of 35,000 cells/mL in 48-well plates (final volume of 250 μL; ~8000 cells/cm^2). After 48 h cells were pre-treated for 30 min, and co-incubated with 1 μM CsA to inhibit the MPTP. After the pre-incubation, cells were incubated with 500, 1000, 1500, and 2000 μM BZP, MeOPP, or MDBP or 50, 100, 250, and 500 μM TFMPP. After 24 h, cell mortality was determined through the MTT reduction assay. The final results were expressed as percentage of control conditions from four independent experiments with each concentration tested in three replicates within each experiment.

2.12. Cell death mode: apoptosis vs necrosis

Cell death analysis was performed by staining H9c2 cells with Annexin V-FITC and propidium iodide (PI) (FITC Annexin V Apoptosis Detection Kit BD Biosciences, USA). Annexin V binds to exposed phosphatidylserine on the plasma membrane of the early apoptotic cells, while late apoptotic and/or necrotic cells are stained by PI. To perform the assay, H9c2 cells were seeded at a density of 12,000 cells/mL in 48-well plates (final volume of 250 μL; ~3,000 cells/cm^2). After 48 h, the cells were incubated with 360 μM BZP, 70 μM TFMPP, 380 μM MeOPP, and 500 μM MDBP. After the 24 h incubation period, the medium was removed, and 100 μL binding buffer was added, followed by 2 μL PI and 3 μL annexin V-FITC. Plates were incubated in the dark at room temperature. After 15 min, the cells were observed under a fluorescence microscope (Nikon, Tokyo, Japan). Five pictures per well were taken, and the percentages of early apoptotic cells were estimated by counting the annexin V-positive but PI-negative cells, whereas the percentages of late apoptotic cells were estimated by counting the number of cells which were both annexin V-positive and PI-positive. Necrotic cells were the PI-positive but annexin V-negative ones. Campthotecin 12 μM was used as a positive control for apoptosis. The results are expressed as percentage cell population from 4 independent experiments.

2.13. Caspase-3 activity assay

Cells were seeded at a density of 35,000 cells/mL in six-well plates (final volume of 2.5 mL, ~9000 cells/cm^2) and allowed to grow. After 48 h, the medium was replaced, and cells were incubated with piperazine designer drugs at 37 °C (1000 and 2000 μM for BZP, MeOPP, or MDBP or 50 and 500 μM for TFMPP). After a 24 h incubation period, the cells were detached and collected to a tube (two wells per tube), centrifuged (210 × *g*, 5 min, 4 °C), and the supernatant was discarded. One hundred and fifty microliters of lysis buffer (50 mM HEPES, 0.1 mM EDTA, 0.1% CHAPS, supplemented with 1 mM DTT, pH 7.4) were added to the pellets, votex-mixed and incubated on ice for 5 min before centrifugation (16,000 × *g*, 10 min, 4 °C). In a 96-well plate, 50 μL of the supernatant, which contains the cytoplasmic fraction, was mixed with 200 μL of assay buffer (100 mM NaCl, 50 mM HEPES, 1 mM EDTA, 0.1% CHAPS, 10% glycerol, supplemented with 10 mM DTT, pH 7.4). The reaction was started by adding 5 μL of caspase-3 peptide substrate Ac-DEVD-pNA (final concentration 80 μM) and subsequent incubation at 37 °C for 24 h. Caspase-3 releases the *p*-nitroaniline moiety of the substrate, which presents high absorbance at 405 nm. All steps were performed on ice, and the caspase-3 activity was determined at 405 nm in a multi-well plate reader (BioTech Instruments, Vermont, US) as previously

described (Barbosa et al., 2014). Caspase-3 substrate Ac-DEVD-pNA (stock solution at 4 mM) and DTT were prepared in DMSO. The absorbance of blanks, used as non-enzymatic control, was subtracted from each value of absorbance. Final results of caspase-3 activity were expressed as optical density at 405 nm/mg of protein. The protein content in the cytoplasmic fraction was quantified using the Bio-Rad DC protein assay kit as described by the manufacturer, and bovine albumin solutions were used as standards. Campthotecin (12 μM) was used as positive control.

2.14. Statistical analysis

Concentration–response curves were obtained from six replicates of each tested concentration from three independent experiments. They were fitted by the least squares method. The comparisons between curves (bottom, top and log EC_{50}) were made using the extra sum-of-squares F test. Results of all other biochemical measures are presented as mean ± standard error of the mean (SEM) from at least three independent experiments. Normality of the data distribution was assessed by the Kolmogorov–Smirnov normality test. Significance was accepted at $p < 0.05$. Statistical comparisons between groups were performed with one-way ANOVA (when data followed normal distribution) or with the Kruskal–Wallis test (one-way ANOVA on ranks in case data distribution was not normal). A two-way ANOVA analysis was conducted when the cells were submitted to a drug challenge after pre-incubation with the MTPT opening inhibitor CsA. Details of the statistical analysis are provided in the text and legend of the figures.

3. Results

3.1. Piperazine designer drugs elicit concentration-dependent cytotoxicity in H9c2 cells

A comprehensive concentration–response analysis was carried out by incubating the H9c2 cells with 0–20 mM of each piperazine designer drug for 24 h. Fig. 2 presents the obtained concentration–response curves showing that in the MTT (A) and NR (B) assays, all tested drugs produced concentration-dependent cytotoxic effects. A summary of the calculated EC_{50} values (representing the half-maximum-effect concentrations from the fitted curves) is presented in Table 1. Significant differences were observed for the EC_{50} values of the curves. Based on these data, it was evident that, under our experimental conditions, TFMPP (EC_{50} 59.6 μM) was the most cytotoxic of the tested piperazine designer drugs to H9c2 cells, followed by BZP (EC_{50} 343.9 μM), MeOPP (EC_{50} 570.1 μM), and MDBP (EC_{50} 702.5 μM). To confirm these results, we also performed the NR uptake assay. The EC_{50} values were higher than those obtained with the MTT assay, but the cytotoxicity profile of the piperazine designer drugs was the same (Table 1, Fig. 2B).

3.2. Oxidative stress does not contribute to the cytotoxic effects elicited by the piperazine designer drugs

Oxidative stress plays an important role in drug-induced cardiotoxicity for many different compounds including drugs of abuse (e.g., cocaine and amphetamines), and pharmaceuticals (e.g., doxorubicin and cyclophosphamide) (Costa et al., 2013). The effect of piperazine designer drugs in the generation of reactive species was, therefore, evaluated by the DCFH-DA assay at different time-points, but no significant changes in reactive species generation were found for any of the tested piperazine drugs even when tested at highly cytotoxic concentrations (data not shown).

Changes in the intracellular amounts of GSH and GSSG are also strong indicators of redox disturbances and were investigated with the DTNB–GSSG reductase recycling assay. In accordance with the data from the DCFH-DA assay, the intracellular GSH levels were not depleted by the piperazine test drugs, even at highly cytotoxic concentrations, with the exception of MDBP. As can be seen in Fig. 3, total GSH levels were significantly decreased ($p < 0.05$, ANOVA/Bonferroni) after 24 h incubations with 1000 and 2000 μM MDBP as compared to control (representing a 23% and 37% decrease, respectively). GSSG was also detected in H9c2 cells: however, no changes in the intracellular levels of the dissulfide were observed for any of the tested drugs (data not shown). Thus, the observed depletions in total GSH levels are probably due to a decrease in reduced GSH intracellular levels as a consequence of

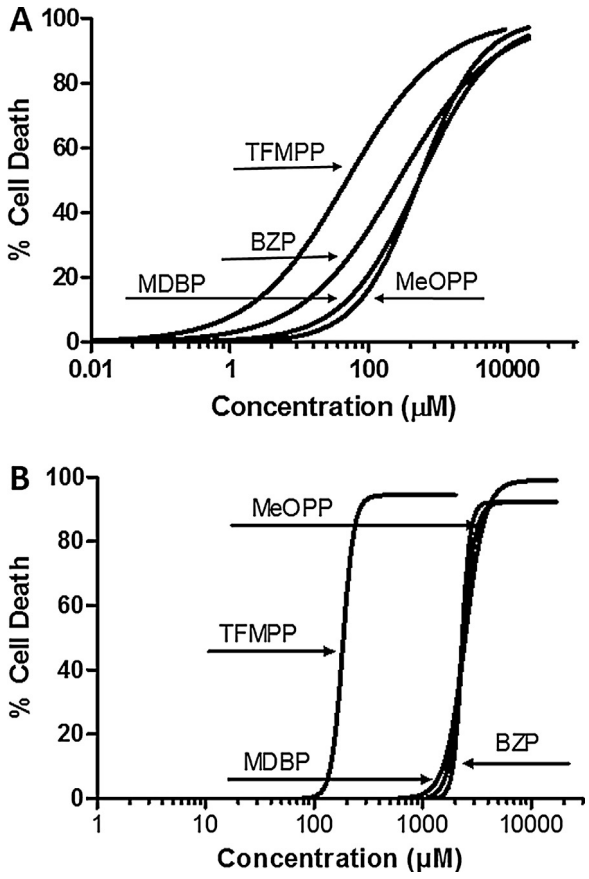

Fig. 2. Concentration–response (cell death) curves of the tested piperazine designer drugs after 24 h incubation in H9c2 cells at 37 °C. Cell viability was evaluated by the MTT reduction (A) and the neutral red uptake (B) assays. Data are presented as percentage of cell death relative to the respective negative controls. Three independent experiments were performed (six replicates tested for each concentration within each experiment). Curves were fitted using least squares as the fitting method.

Table 1
EC_{50} values of the piperazine designer drugs.

Designer drug	EC_{50} MTT (μM)	EC_{50} NR (μM)
BZP	343.9	2332[b]
TFMPP	59.6[a]	186.4[a,c,d]
MeOPP	570.1[a,b]	2366[b]
MDBP	702.5[a,b]	2469[b]

The cytotoxicity curves were fitted using least squares as the fitting method. Comparisons were made using the extra sum-of-squares F test ($p < 0.05$).
[a] Compares to BZP.
[b] Compares to TFMPP.
[c] Compares to MeOPP.
[d] Compares to MDBP.

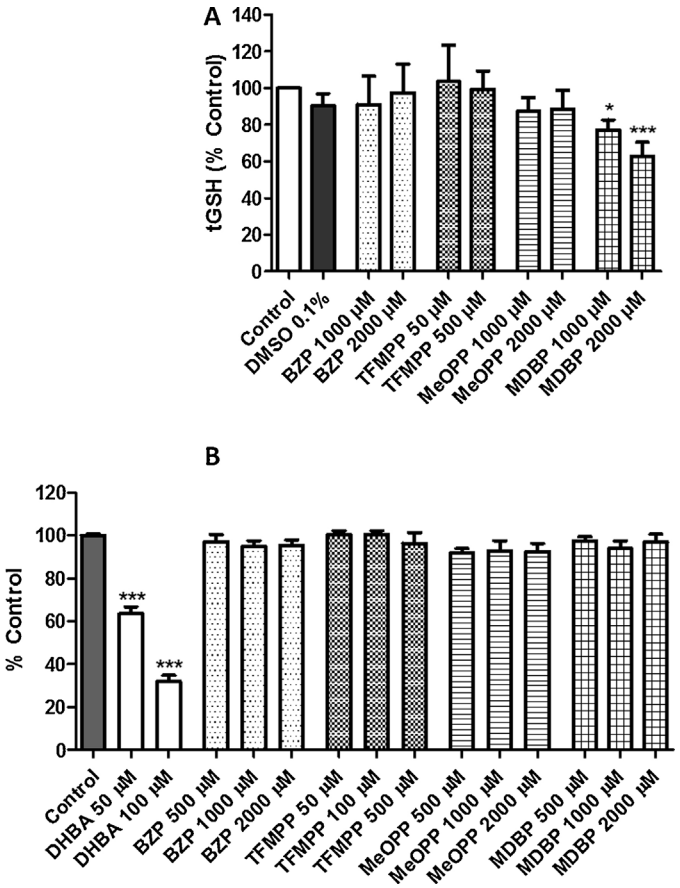

Fig. 3. (A) Intracellular contents of total glutathione (tGSH) in H9c2 cells after 24 h incubations with the tested piperazine designer drugs at 37 °C. (B) Effect of piperazine designer drugs in the activity of GSH reductase (GR). Results are expressed as percentage control ± SEM ($n = 5$ independent experiments run in triplicates). Statistical comparisons were made using one-way ANOVA/Bonferroni post-hoc test ($^{*}p < 0.05$; $^{***}p < 0.001$ vs control).

the metabolic bioactivation of MDBP into reactive metabolites that can conjugate GSH but an interference with the enzymes involved in GSH homeostasis, namely with glutathione reductase (GR), cannot be discarded. To test this hypothesis, the influence of the piperazine designer drugs on the activity of the GR enzyme was measured, and no differences were found at the concentration range tested (Fig. 3B).

3.3. Piperazine designer drugs disturb the cellular energetic status and Ca^{2+} homeostasis

ATP, the key intermediate for energy exchange, is engaged in a variety of cellular activities, including cellular energetics, metabolic regulation, and signalling. Since all cells require ATP to remain alive and carry out their specific functions and, because ATP is transiently depressed by many forms of cellular stress, its levels reflect the functional integrity of viable cells. Fig. 4 shows that the ATP levels measured in H9c2 cells after 24 h incubations with the tested piperazine designer drugs at 37 °C were significantly depleted at highly cytotoxic concentrations. Significant ($p < 0.05$, ANOVA/Bonferroni) 23 and 45% decreases in ATP levels in relation to negative controls were observed at 1000 and 2000 μM BZP. For 500 μM TFMPP, a 45% decrease was noted, while this decrease was of 28% for 2000 μM MeOPP, and 27% and 35%, respectively, for 1000 and 2000 μM MDBP.

Intracellular Ca^{2+} homeostasis is also critical for maintaining the normal function of the cell, in that variations in the

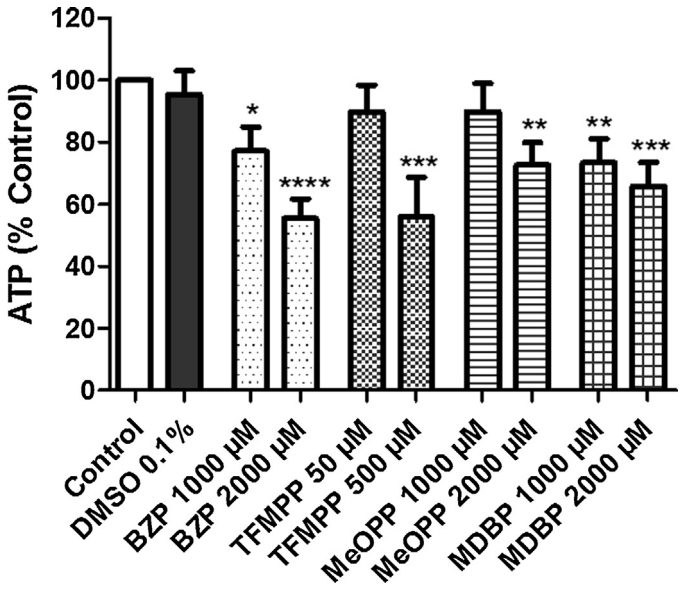

Fig. 4. Intracellular contents of ATP in H9c2 cells after 24 h incubations with the tested piperazine designer drugs at 37 °C. Results are expressed as percentage control ± SEM ($n = 5$ independent experiments run in duplicates). Statistical comparisons were made using one-way ANOVA/Bonferroni post-hoc test ($^{*}p < 0.05$; $^{**}p < 0.01$; $^{***}p < 0.001$; $^{****}p < 0.0001$ vs control).

concentration of Ca^{2+} in cells can determine cell survival or death (Oliveira and Gonçalves, 2009). Incubation with piperazine designer drugs significantly increased ($p < 0.05$, Kruskal–Wallis) the intracelular Ca^{2+} levels in a concentration-dependent manner. As shown in Fig. 5, a 37% increase occured at 1000 μM BZP in relation to negative controls. At 50 and 100 μM TFMPP, mean fluorescence markedly increased up to 89% and 123% over control values, respectively. At 500 μM MeOPP and 1000 μM MDBP increases of 130% and 118% relative to control, respectively, could also be observed.

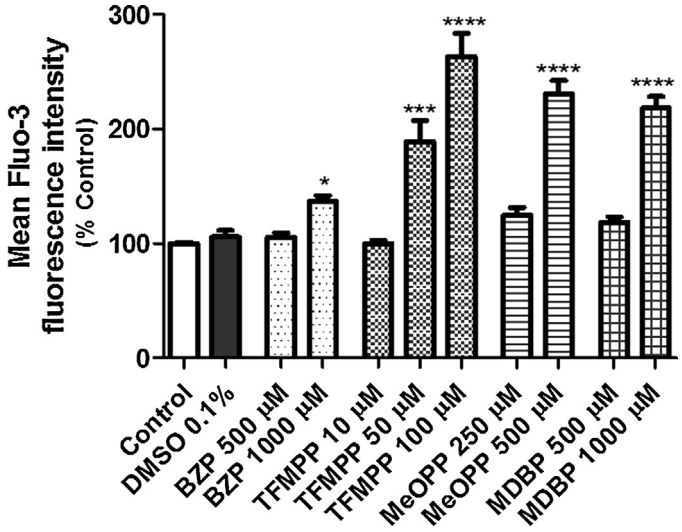

Fig. 5. Intracellular levels of Ca^{2+} in H9c2 cells after 24 h incubations with the tested piperazine designer drugs at 37 °C. Results are expressed as percentage control ± SEM ($n = 6$ independent experiments run in duplicates). Statistical comparisons were made using the non-parametric Kruskal–Wallis test ($^{*}p < 0.05$; $^{***}p < 0.001$; $^{****}p < 0.0001$ vs control).

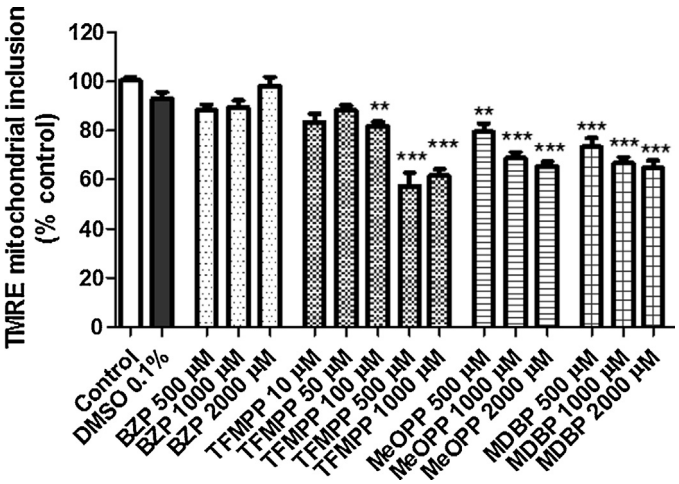

Fig. 6. Mitochondrial membrane potential (Δψm) measured as TMRE incorporation in mitochondria of H9c2 cells after 24 h incubations with the tested piperazine designer drugs at 37 °C. Results are expressed as percentage control ± SEM ($n = 6$ independent experiments run in triplicates). Statistical comparisons were made using one-way ANOVA/Bonferroni post-hoc test (**$p < 0.01$; ***$p < 0.001$ vs control).

3.4. Mitochondrial function is severely affected by the piperazine designer drugs

To investigate whether the piperazine drugs could disturb the mitochondrial function, the mitochondrial membrane potential (Δψm) was evaluated. A significant loss of Δψm impairs oxidative phosphorylation, depleting cells of energy, and inducing cell death. In Fig. 6, a significant loss in Δψm ($p < 0.01$, ANOVA/Bonferroni) can be observed after 24 h incubations of H9c2 cells with 100, 500, and 1000 μM TFMPP (with decreases of 18, 43 and 39%, respectively) in relation to control values. At 500, 1000, and 2000 μM MeOPP, this loss comprises 21, 33, and 35% of control Δψm, while 27, 33, and 36% decreases in Δψm relative to control occurred at 500, 1000, and 2000 μM MDBP, respectively. BZP did not produce any measurable modifications in Δψm even at highly cytotoxic concentrations.

Increase of intracellular Ca^{2+} levels, loss of Δψm, and ATP depletion are indicative signals of MPTP opening. Fig. 7 shows the involvement of MPTP in the cytotoxic effects of the tested piperazine designer drugs. When the H9c2 cells were incubated with the tested drugs in the presence of 1 μM cyclosporine A (CsA) (including a pre-incubation period of 30 min), it was possible to observe a partial reversion of the piperazine designer drugs cytotoxic effects. In fact, the cytotoxic effects produced by 1500 and 2000 μM BZP after pre-incubation with 1 μM CsA were significantly lower ($p < 0.05$, ANOVA/Bonferroni) than those observed in the absence of CsA. In these set of experiments, the BZP control incubations without CsA revealed lower toxicity levels than those expected from the cytotoxicity curves, but this is likely explained by the steepness of the MTT cytotoxicity assay curve at these concentration ranges. The cells incubated with 50, 100, 250, and 500 μM TFMPP presented a significant ($p < 0.001$, ANOVA/Bonferroni) cytotoxic effect in the MTT assay. The incubation with CsA 1 μM was capable to slightly but significantly increase cell survival at the tested 50 and 100 μM TFMPP concentrations. However, the protective effects of CsA were not observed for the higher and more cytotoxic TFMPP concentrations. Incubation with MeOPP also resulted in a significant ($p < 0.001$, ANOVA/Bonferroni) cell death. CsA was able to significantly ($p < 0.05$, ANOVA/Bonferroni) increase cell survival only at 2000 μM MeOPP. The

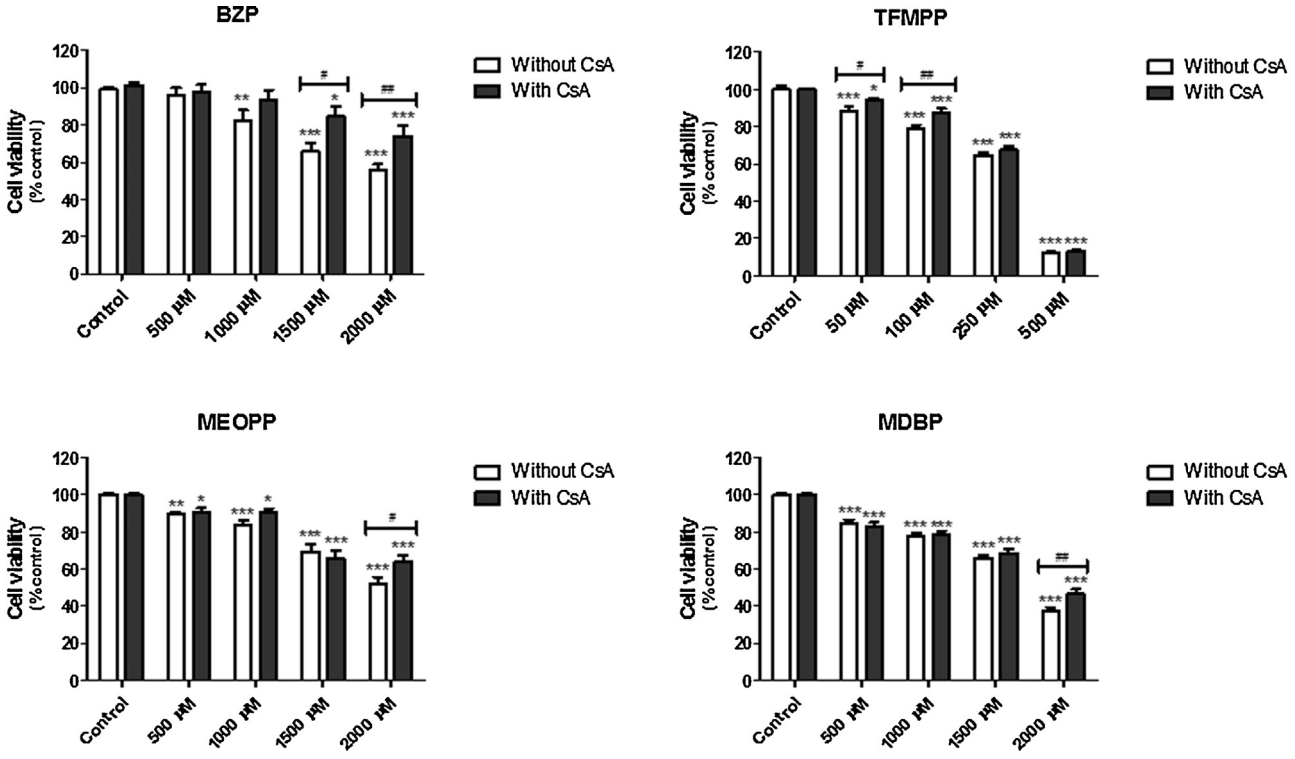

Fig. 7. Involvement of the mitochondrial permeability transition pore (MPTP) in the piperazine designer drugs-induced cell death. Viability was evaluated by the MTT reduction assay in H9c2 cells after 24 h incubations with the tested piperazine designer drugs with and without 30 min pre-incubation followed by co-incubation with 1 μM cyclosporine A (CsA) at 37 °C. Results are expressed as percentage control ± SEM ($n = 4$ independent experiments run in triplicates). Statistical comparisons were made using two-way ANOVA/Bonferroni post-hoc test, for comparisons vs the respective control condition (*$p < 0.05$; **$p < 0.01$; ***$p < 0.001$ vs control) and for comparison between the same concentration with or without 1 μM CsA (#$p < 0.05$; ##$p < 0.01$ vs incubation without 1 μM CsA).

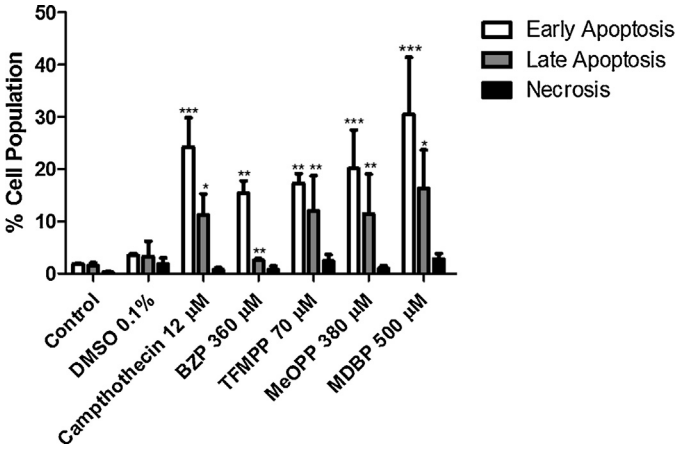

Fig. 8. Annexin V/PI staining of H9c2 cells after 24 h incubations with the tested piperazine designer drugs at 37 °C. The H9c2 cell population was divided into early apoptotic (annexin V+/PI−), late apoptotic (annexin V+/PI+), and necrotic (annexin V−/PI+) cells. Results are expressed as percentage cell population ± SEM ($n = 4$ independent experiments). Statistical comparisons were made using one-way ANOVA/Bonferroni post-hoc test (*$p < 0.05$; **$p < 0.01$; ***$p < 0.001$ vs control).

incubation with 1 μM CsA was also able to increase cell viability after MDBP incubations but only at the highest 2000 μM tested concentration of the drug. In spite of the observed increases in survival, cell viability after CsA incubations was still significantly lower than control ($p < 0.05$, ANOVA/Bonferroni).

In order to evaluate the mode of death, the cells were stained with annexin V-FITC and PI after 24 h incubations with the piperazine designer drugs at concentrations that approximately corresponded to their EC_{50} levels, as determined by the MTT assay. Fig. 8 depicts the relative number (percentage of cell population) of early apoptotic, late apoptotic (undergoing secondary necrosis) and necrotic H9c2 cells. At the tested concentrations, after incubation with all piperazine test drugs a high number of cells presenting early apoptosis features, i.e., stained only with annexin V-FITC could be observed relative to the control cell population (Fig. S1, Supplemented material). A high number of cells that were double-stained with both annexin V-FITC and PI were also found after the drug incubations. These cells are likely undergoing secondary necrosis and present features of both types of cell death. The number of necrotic cells did not significantly differ from control cells for any of the piperazine designer drugs.

Supplementry material related to this article found, in the online version, at http://dx.doi.org/10.1016/j.toxlet.2014.06.031.

Notwithstanding, when the activation of caspase-3, that is involved in the apoptotic cascade, was investigated, no significant changes in this downstream effector caspase activity were observed after 24 h incubations (data not shown).

4. Discussion

A recent survey in the UK found that piperazines are among the most common active recreational drugs in tablets purchased from internet supplier sites (Davies et al., 2010). These so-called party pills gained popularity in the 2000s as a legal and arguably safer alternative to MDMA. However, the available information on the toxic effects of piperazine designer drugs is currently very limited.

For the first time, we demonstrate that piperazine designer drugs produce cytotoxicity to H9c2 cells, a commercially available myogenic cell line derived from embryonic rat heart ventricle that has been considered suitable for the study of drug-induced cardiotoxicity (Watkins et al., 2011), specially due to their metabolic competence that parallels the metabolic capacity of the heart (Zordoky and El-Kadi, 2007). Among the four tested piperazine designer drugs, TFMPP was the most potent drug to elicit cytotoxic effects. This is in accordance with the cardiovascular effects experienced by users (Wood et al., 2008; Kovaleva et al., 2008; Gee et al., 2010). In this work, we used two viability tests, the MTT reduction and the NR uptake assays, to determine the cytotoxicity of the piperazine designer drugs. In spite of the differences in the obtained EC_{50} values, the cytotoxicity profile of the drugs was the same for the two tests. Discrepancies among different viability tests are quite commonly noted in the literature (Putnam et al., 2002; Weyermann et al., 2005; Pohjala et al., 2007; Kim et al., 2009; Zwolak, 2013). The main difference between these two assays is that MTT measures the activity of succinate dehydrogenase, which is present in the mitochondrial inner membrane (Putnam et al., 2002), while NR is based on the storage of NR dye in the lysosomes and probably in the golgi apparatus (Zwolak, 2013). Any damage to lysosomes/golgi apparatus decreases the cellular accumulation of the dye. On the other hand, mitochondrial succinate dehydrogenase is sensitive to local changes in ion concentrations and ion flux. It is not uncommon for some chemicals to increase metabolic activity in a cell, which would result in increased mitochondrial succinate dehydrogenase activity (Putnam et al., 2002). Also, MTT does not seem to be appropriate for the evaluation of cytotoxicity in cells with an unchanged reduction fluctuation by a high level of basal cellular reduction capacity and/or oxidant defense (Kim et al., 2009). In the present case, oxidative stress does not seem to contribute to the toxic effect of piperazine designer drugs in H9c2 cells, and the piperazine derivatives alter ionic concentration through the disruption of Ca^{2+} homeostasis. Therefore, MTT is probably not the best test for evaluation the cytotoxicity of the piperazine designer drugs. Accordingly, the NR cytotoxicty data agree much better with the oxidative stress and energetic imbalance endpoints additionally measured, while the MTT seems to overestimate the cytotoxic potential of the piperazine designer drugs.

Oxidative stress is a well-described mechanism underlying the toxicity of many xenobiotics, which plays an essential role in the cytotoxic effects of several amphetamine derivatives that induce the formation of highly reactive species (Dias da Silva et al., 2013b). Interestingly, piperazine designer drugs failed to induce reactive species formation, as measured through the DCFH-DA assay. GSH has an important protective role which involves its oxidant neutralizing and lipid peroxidase and/or tocopheryl radical-regenerating activities. Changes in the intracellular amounts of GSH and GSSG are, therefore, strong indicators of redox disturbances. In agreement with the DCFH-DA assay data, the intracellular GSH level remained significantly unchanged upon incubation with the piperazine designer drugs with the exception of MBDP. Our data indicate a decrease in intracelular tGSH content after incubation with MDBP for 24 h. However, these decreases were not accompanied by significant alterations in GSSG levels or inhibition of the GR enzymatic activity. A possible explanation for this result is that the GSSG formed through the free radicals neutralizing reactions of GSH could be extruded for the extracellular medium, contributing to the decrease in the tGSH levels. This GSSG efflux is a cellular response that protects the cells from oxidative stress (Rossato et al., 2011). However, since no formation of reactive species could be observed, it is not likely that the observed depletion in tGSH levels is due to increased GSSG formation. Depletion may be caused by inhibition of GSH biosynthesis (Gao et al., 2010), which occurs in the cytosol, and involves two enzymes: γ-glutamylcysteine ligase and GSH synthase, the first catalyzing the rate-limiting step of this biosynthetic pathway (Marí et al., 2013). A key role in GSH homeostasis is also played by γ-glutamyl transpeptidase (GGT), which breaks down extracellular GSH and provides cysteine, the rate-limiting substrate, for intracellular de novo synthesis of GSH

(Zhang et al., 2005). Another pathway involves the reduction of GSSG by GR producing two molecules of GSH. GR is known to be sensitive to chemical modification of its active thiol groups. Thus, the activity of GR can be modulated by the redox conditions of the reactive environment. Under extreme oxidising conditions, aggregates of GR may be formed, which decrease GR activity (Remião et al., 2000). However, according to our results, the piperazine designer drugs do not seem to have any influence on the GR activity.

In fact, it has been previously described that the cardiotoxicity of MDMA involves the formation of catechol metabolites that are oxidized into quinone intermediates following the demethylenation of MDMA (Hiramatsu et al., 1990) and methylenedioxyamphetamine (MDA) (Carvalho et al., 2004) leading to the production of the corresponding glutathione-*S*-yl-*N*-methyl-α-methyldopamine and glutathione-*S*-yl-α-methyldopamine conjugates. There is a striking similarity with the main metabolic pathways that were already described for MDBP in animals and in humans, namely the demethylenation of MDBP (Staack and Maurer, 2004), which can lead to the formation of similar GSH adducts, since a catechol intermediate is also formed. Although such conjugate formation is yet to be demonstrated, this possible metabolic bioactivation affords an alternative and reasonable explanation for the GSH decreases that were observed with only MDBP.

Cardiac myocytes are endowed with high content of mitochondria, equivalent to approximately 30% of the cellular volume, and maintain an elevated rate of ATP synthesis to satisfy the energy demand of the heart (Lax et al., 2009). Depletion of ATP is a typical feature of hypoxic and toxic injury and could be due to an alteration in mitochondrial function. Indeed, mitochondria seems to play an essential role in piperazine designer drugs-induced cardiotoxicity. Mitochondria is generally considered the 'powerhouse' of the cell in generating ATP, but they also play an important role in other aspects of normal cell functioning. Apart from ATP synthesis, mitochondrial Ca^{2+} uptake represents a major function of mitochondria; thus, regulating Ca^{2+}-dependent signalling pathways (Griffiths, 2000). Ca^{2+} uptake is driven by the electrochemical potential gradient generated by the combination of the $\Delta\psi m$ and the low concentration of Ca^{2+} in the matrix (Duchen, 1999). It is well established that mitochondria accumulate Ca^{2+} ions during cytosolic Ca^{2+} elevations in a variety of cell types including cardiomyocytes (Kumar et al., 2012). The downward electrochemical gradient across the inner membrane directs Ca^{2+} into the mitochondria through an uniporter. If mitochondrial buffering capacity is overwhelmed by elevated Ca^{2+}, mitochondrial matrix Ca^{2+} increases to levels high enough to trigger the opening of the mitochondrial permeability transition pore (MPTP). This involves the formation of pores in the inner membranes of pores with $\leq$1.5 kDa, allowing the influx of water and solutes into the matrix. Although MPTP can 'flicker' and be reversible, sustained transitions lead to the collapse of $\Delta\psi m$, cessation of ATP production, and cell death (Dong et al., 2006). Disruptions in Ca^{2+} homeostasis may abnormally alter myocardial excitability and contractility and induce arrhythmia or ventricular fibrillation. Increased intracellular Ca^{2+} may also affect signalling pathways, leading to diverse responses including fibrosis and hypertrophy (Tiangco et al., 2005).

Our data show that piperazine designer drugs alter the Ca^{2+} homeostasis, leading to an increase in cytosolic free Ca^{2+} levels, observed with 1000 μM BZP and MDBP, 500 μM MeOPP, and 50 μM TFMPP. At higher concentrations, the mitochondria buffering capacity was overwhelmed and led to the loss of $\Delta\psi m$ and mitochondrial depolarization and the depletion of ATP. In response to mitochondrial depolarization, the ATP synthase reverts to an ATPase activity, consuming ATP and pumping protons outwards, in a futile, energy consuming cycle (Duchen, 1999). According to the chemiosmotic theory of mitochondrial oxidative phosphorylation, $\Delta\psi m$ is the driving force behind oxidative phosphorylation. Thus, maintenance of $\Delta\psi m$ is extremely important for normal cell function (Mathur et al., 2000). Generation of $\Delta\psi m$ depends on a proton gradient across the inner mitochondrial membrane. It is known that translocation of protons from the matrix to the intermembrane space to establish $\Delta\psi m$ is coupled to the mitochondrial electron transport chain (Yuan and Acosta, 1996). Inhibition of chain activity undoubtedly diminishes $\Delta\psi m$, and this could be another pathway through which piperazine designer drugs decrease cellular energy and impair mitochondrial function. Using the same H9c2 cellular model, other studies conducted with MDMA, a drug which mimics the piperazine designer drugs effects, similarly demonstrated the involvement of increased intracellular Ca^{2+} concentrations and loss of $\Delta\psi m$ in the cytotoxic effects of the drug (Tiangco et al., 2005).

Since these results suggest the involvement of MPTP in these cytotoxic events, we pre-incubated cells with CsA and then further incubated the piperazines designer drugs in the presence of CsA. Cyclosporin A binds to cyclophilin D, part of the MPTP, causing inhibition of the MPTP opening and preventing cell death (Crompton, 1999). The incubations with CsA only partially, but significantly, prevented cell death induced by the tested piperazine drugs. It is plausible that the inhibition of MPTP open did not block Ca^{2+} influx and, therefore, did not prevent the alteration in the electron gradient across the inner membrane. Also, Ca^{2+} may possibly enter the matrix through alternative pathways other than the Ca^{2+} uniporter. Recently, growing bodies of evidence of other mechanisms related to the mitochondrial Ca^{2+} influx have been reported. These mechanisms involve the mitochondrial ryanodine receptor, a rapid mode of Ca^{2+} uptake, mitochondrial uncoupling proteins, and leucine zipper EF hand-containing transmembrane protein 1 (LETM1) Ca^{2+}/H^{+} antiporter. Ca^{2+} influx through these alternative Ca^{2+} uptake channels could also trigger MPTP opening (Yarana et al., 2012).

MPTP opening generally represents a catastrophe for the cell and will lead inexorably to cell death, either through ATP consumption, acute energy failure and necrosis or through the initiation of apoptosis (Duchen, 1999). Whereas the loss of ion homeostasis resulting from ATP depletion can lead to necrosis, MPTP opening also causes a leakage of cytochrome c from mitochondria, and thus, triggers a cascade of events that eventually lead to apoptosis (Chiu et al., 2008). Apoptotic cells are characterized by a set of distinct morphological changes, which can be classified as early and late apoptotic changes. The early marker of apoptosis is the exposition of phosphatidilserine on the cell surface (it is normally concentrated in the luminal layer of the cytoplasmic membrane), while, at the later stage, the entire phosphatidylserine is flipped on the outer membrane (Kumar et al., 2012). When the rate of apoptosis is substantially increased, the cells undergo secondary necrosis (or late apoptosis) with breakdown of membrane potential, cell swelling and cell contents release. These cells present features of both the apoptotic and necrotic cells and in many cases can only be accurately distinguished with detailed morphological analysis. When the mode of cell death was investigated, we found an unexpected high number of cells that were at an early apoptotic stage and a low number of necrotic cells. However, an elevated number of cells that were double-stained and most likely undergoing secondary necrosis was also noted for all the piperazine drugs; thus, agreeing with the previous data that clearly indicated a preferential necrotic cell death pathway characterized by the loss of $\Delta\psi m$, ATP depletion and MPTP opening. Accordingly, under our experimental conditions, we did not observe any activation of downstream effector caspase-3,

which also suggests that necrotic cell death would predominate. However, alternative mechanisms for apoptosis induction that are independent of caspases activation have been described. In fact, activation of calpains due to increased intracellular Ca^{2+} concentrations has been linked to cardiomyocyte death. A mechanism for ceramide-induced cardiomyocyte death with apoptosis induction, which can turn into necrosis, following ATP depletion, increased Ca^{2+} influx, mitochondrial network fragmentation and loss of the mitochondrial Ca^{2+} buffer capacity dependent on calpains activation and independent of caspases or reactive species production has been described (Parra et al., 2013). Nevertheless, the involvement of apoptotic and necrotic pathways should be further investigated for a better comprehension of the cell death mechanisms involved in the cytotoxicity of the piperazine designer drugs.

In conclusion, we describe, for the first time, the cardiotoxic effects of piperazine designer drugs in an in vitro model. Among the tested designer drugs, TFMPP was the most potent in inducing cytotoxicity. In H9c2 cells, piperazine designer drugs induced cell death by causing disturbances in Ca^{2+} homeostasis, ATP depletion, loss of $\Delta\psi m$ and MPTP opening. It should be noted that these drugs are frequently consumed in associations, such as TFMPP with BZP or BZP/TFMPP with MDMA, often in the same tablet. As previously observed with amphetamine designer drugs, marked toxicity can occur when the drugs are combined at individually non-cytotoxic concentrations (Dias da Silva et al., 2013a, 2013b, 2013c). Since combinations of piperazine designer drugs have already been implicated in human intoxications, further studies are needed not only to clarify the mechanisms involved in the observed cytotoxic effects of the isolated drugs but also to address the effects of such drug combinations.

Conflict of interest

The authors declare that there are no conflicts of interest.

Transparency document

The Transparency document associated with this article can be found in the online version.

Acknowledgements

Marcelo Dutra Arbo is the recipient of Coordenação de Aperfeiçoamento de Pessoal de Nível Superior (CAPES Foundation – Brazil) fellowship (Proc. BEX 0593/10-9). Renata Silva, Daniel José Barbosa and Luciana Grazziotin Rossato, were supported by fellowships (SFRH/BD/29559/2006, SFRH/BD/64939/2009 and SFRH/BD/63473/2009, respectively) from Fundação para a Ciência e Tecnologia (FCT), Portugal. This work was sponsored by the Portuguese Research Council Fundação para a Ciência e para a Tecnologia (FCT) [Grant No. PEst-C/EQB/LA0006/2011] and co-funded by the European Community Financial Support Program "Programa Operacional Factores de Competitividade do Quadro de Referência Estratégico Nacional (QREN POFC)".

References

Antia, U., Lee, H.S., Kydd, R.R., Tingle, M.D., Russell, B.R., 2009. Pharmacokinetics of 'party pill' drug *N*-benzylpiperazine (BZP) in healthy human participants. Forensic Sci. Int. 186, 63–67.

Antia, U., Tingle, M.D., Russel, B.R., 2010. Validation of an LC-MS method for the detection and quantification of BZP and TFMPP and their hydroxylated metabolites in human plasma and its application to the pharmacokinetic study of TFMPP in humans. J. Forensic Sci. 55, 1311–1318.

Arbo, M.D., Bastos, M.L., Carmo, H., 2012. Piperazine compounds as drugs of abuse. Drug Alcohol Depend. 122, 174–185.

Austin, H., Monasterio, E., 2004. Acute psychosis following ingestion of 'Rapture'. Australas. Psychiatry 12, 406–408.

Barbosa, D.J., Capela, J.P., Silva, R., Ferreira, L.M., Branco, P.S., Fernandes, E., Bastos, M. L., Carvalho, F., 2014. "Ecstasy"-induced toxicity in SH-SY5Y differentiated cells: role of hyperthermia and metabolites. Arch. Toxicol. 88, 515–531.

Carvalho, M., Carmo, H., Costa, V.M., Capela, J.P., Pontes, H., Remião, F., Carvalho, F., Bastos, M.L., 2012. Toxicity of amphetamines: an update. Arch. Toxicol. 86, 1167–1231.

Carvalho, M., Remião, F., Milhazes, N., Borges, F., Fernandes, E., Monteiro do, M.C., Gonçalves, M.J., Seabra, V., Amado, F., Carvalho, F., Bastos, M.L., 2004. Metabolism is required for the expression of ecstasy-induced cardiotoxicity in vitro. Chem. Res. Toxicol. 17, 623–632.

Chiu, P.Y., Luk, K.F., Leung, H.Y., Ng, K.M., Ko, K.M., 2008. Schisandrin B stereoisomers protect against hypoxia/reoxygenation-induced apoptosis and inhibit associated changes in Ca^{2+}-induced mitochondrial permeability transition and mitochondrial membrane potential in H9c2 cardiomyocytes. Life Sci. 82, 1092–1101.

Costa, V.M., Carvalho, F., Duarte, J.A., Bastos, M.L., Remião, F., 2013. The heart as a target for xenobiotic toxicity: the cardiac susceptibility to oxidative stress. Chem. Res. Toxicol. 26, 1285–1311.

Crompton, M., 1999. The mitochondrial permeability transition pore and its role in cell death. Biochem. J. 341, 233–249.

Davies, S., Wood, D.M., Smith, G., Button, J., Ramsey, J., Archer, R., Holt, D.W., Dargan, P.I., 2010. Purchasing 'legal highs' on the internet – is there consistency in what you get? QJM 103, 489–493.

Dawson, P., Moffatt, J.D., 2012. Cardiovascular toxicity of novel psychoactive drugs: lessons from the past. Prog. Neuro-Psychopharmacol. Biol. Psychiatry 39, 244–252.

Dias da Silva, D., Carmo, H., Silva, E., 2013a. The risky cocktail: what combination effects can we expect between ecstasy and other amphetamines? Arch. Toxicol. 87, 111–122.

Dias da Silva, D., Silva, E., Carmo, H., 2013c. Combination effects of amphetamines under hyperthermia – the role played by oxidative stress. J. Appl. Toxicol. doi: http://dx.doi.org/10.1002/jat.2889.

Dias da Silva, D., Carmo, H., Lynch, A., Silva, E., 2013b. An insight into hepatocellular death induced by amphetamines, individually and in combination: the involvement of necrosis and apoptosis. Arch. Toxicol. 87, 2165–2185.

Dong, Z., Saikumar, P., Weinberg, J.M., Venkatachalam, M.A., 2006. Calcium in cell injury and death. Annu. Rev. Pathol. Mech. Dis. 1, 405–434.

Duchen, M.R., 1999. Contributions of mitochondria to animal physiology: from homeostatic sensor to calcium signalling and cell death. J. Physiol. 516, 1–17.

Feuchtl, A., Bagli, M., Stephan, R., Frahnert, C., Kölsch, H., Kühn, K.U., Rao, M.L., 2004. Pharmacokinetics of m-chlorophenylpiperazine after intravenous and oral administration in healthy male volunteers: implication for the pharmacodynamic profile. Pharmacopsychiatry 37, 180–188.

Gao, W., Mizukawa, Y., Nakatsu, N., Minowa, Y., Yamada, H., Ohno, Y., Urushidani, T., 2010. Mechanism-based biomarker gene sets for glutathione depletion-related hepatotoxicity in rats. Toxicol. Appl. Pharmacol. 247, 211–221.

Gee, P., Gilbert, M., Richardson, S., Moore, G., Paterson, S., Graham, P., 2008. Toxicity from the recreational use of 1-benzylpiperazine. Clin. Toxicol. 46, 802–807.

Gee, P., Jerram, T., Bowie, D., 2010. Multiorgan failure from 1-benzylpiperazine ingestion – legal high or lethal high? Clin. Toxicol. 48, 230–233.

Gee, P., Richardson, S., Woltersdorf, W., Moore, G., 2005. Toxic effects of BZP-based herbal party pills in humans: a prospective study in Christchurch, New Zealand. NZ Med. J. 118, 1784–1794.

Gijsman, H.J., Van Gerven, J.M.A., Tieleman, M.C., Schoemaker, R.C., Pieters, M.S.M., Ferrari, M.D., Cohen, A.F., Van Kempen, G.M.J., 1998. Pharmacokinetic and pharmacodynamic profile of oral and intravenous meta-chlorophenylpiperazine in healthy volunteers. J. Clin. Psycopharmacol. 18, 289–295.

Griffiths, E.J., 2000. Mitochondria – potential role in cell life and death. Cardiovasc. Res. 46, 24–27.

Hiramatsu, M., Kumagai, Y., Unger, S.E., Cho, A.K., 1990. Metabolism of methylenedioxymethamphetamine: formation of dihydroxymethamphetamine and a quinone identified as its glutathione adduct. J. Pharmacol. Exp. Ther. 254, 521–527.

Kim, H., Toon, S.C., Lee, T.Y., Jeong, D., 2009. Discriminative cytotoxicity assessment based on various cellular damages. Toxicol. Lett. 184, 13–17.

Kimes, B.W., Brandt, B.L., 1976. Properties of a clonal muscle cell line from rat heart. Exp. Cell Res. 98, 367–381.

Kovaleva, J., Devuyst, E., De Paepe, P., Verstraete, A., 2008. Acute chlorophenylpiperazine overdose: a case report and review of the literature. Ther. Drug Monit. 30, 394–398.

Kumar, S., Kain, V., Sitasawad, S.L., 2012. High glucose-induced Ca^{2+} overload and oxidative stress contribute to apoptosis of cardiac cells through mitochondrial dependent and independent pathways. Biochim. Biophys. Acta 1820, 907–920.

Labonne, B.E.F., Gutiérrez, M., Gómez-Quiroz, L.E., Fainstein, M.K., Bucio, L., Souza, V., Flores, O., Ortíz, V., Hernández, E., Kershenobich, D., Gutiérrez-Ruiz, M.C., 2009. Acetaldehyde-induced mitochondrial dysfunction sensitizes hepatocytes to oxidative damage. Cell Biol. Toxicol. 25, 599–609.

Lax, A., Soler, F., Fernández-Belda, F., 2009. Mitochondrial damage as death inducer in heart-derived H9c2 cells: more than one way for an early demise. J. Bioenerg. Biomembr. 41, 369–377.

Lin, J.C., Bangs, N., Lee, H.S., Kydd, R.R., Russell, B.R., 2009. Determining the subjective and physiological effects of BZP on human females. Psychopharmacology (Berl.) 207, 439–446.

Lin, J.C., Jam, R.K., Lee, H.S., Jensen, M.A., Kydd, R.R., Russell, B.R., 2011. Determining the subjective and physiological effects of BZP combined with TFMPP in human males. Psycopharmacology 214, 761–768.
Marí, M., Morales, A., Colell, A., García-Ruiz, C., Kaplowitz, N., Fernández-Checa, J.C., 2013. Mitochondrial glutathione: features, regulation and role in disease. Biochim. Biophys. Acta 1830, 3317–3328.
Maurer, H.H., Kraemer, T., Springer, D., Staack, R.F., 2004. Chemistry, pharmacology, toxicology and hepatic metabolism of designer drugs of the amphetamine (ecstasy), piperazine, and pyrrolidinophenone types. Ther. Drug Monit. 26, 127–131.
Mathur, A., Hong, Y., Kemp, B.K., Barrientos, A.A., Erusalimsky, J.D., 2000. Evaluation of fluorescent dyes for the detection of mitochondrial membrane potential changes in cultured cardiomyocytes. Cardiovasc. Res. 46, 126–138.
Oliveira, J.M.A., Gonçalves, J., 2009. In situ mitochondrial Ca^{2+} buffering diferences of intact neurons and astrocytes from cortex and striatum. J. Biol. Chem. 284, 5010–5020.
Parra, V., Moraga, F., Kuzmicic, J., López-Crisosto, C., Troncoso, R., Torrealba, N., Criollo, A., Díaz-Elizondo, J., Rothermel, B.A., Quest, A.F.G., Lavandero, S., 2013. Calcium and mitochondrial metabolism in ceramide-induced cardiomyocyte death. Biochim. Biophys. Acta 1832, 1334–1344.
Pohjala, L., Tammela, P., Samanta, S.W., Yli-Kauhaluoma, J., Vuorela, P., 2007. Assessing the data quality in predictive toxicology using a panel of cell lines and cytotoxicity assays. Anal. Biochem. 362, 221–228.
Putnam, K.P., Bombick, D.W., Doolittle, D.J., 2002. Evaluation of eight in vitro assays for assessing the cytotoxicity of cigarette smoke condensate. Toxicol. in Vitro 16, 599–607.
Rao, K.M., Padmanabhan, J., Kilby, D.L., Cohen, H.J., Currie, M.S., Weinberg, J.B., 1992. Flow cytometric analysis of nitric oxide production in human neutrophils using dichlorofluorescein diacetate in the presence of a calmodulin inhibitor. J. Leukocyte Biol. 51, 496–500.
Remião, F., Carmo, H., Carvalho, F.D., Bastos, M.L., 2000. Inhibition of glutathione reductase by isoproterenol oxidation products. J. Enzym. Inhib. 15, 47–61.
Rossato, L.G., Costa, V.M., de Pinho, P.G., Carvalho, F., de Lourdes Bastos, M., Remião, F., 2011. Structural isomerization of synephrine influences its uptake and ensuing glutathione depletion in rat-isolated cardiomyocytes. Arch. Toxicol. 85, 929–939.
Rossato, L.G., Costa, V.M., Vilas-Boas, V., Bastos, M.L., Rolo, A., Palmeira, C., Remião, F., 2013. Therapeutic concentrations of mitoxantrone elicit energetic imbalance in H9c2 cells as an earlier event. Cardiovasc. Toxicol. 13, 413–425.
Scaduto Jr, R.C., Grotyohann, L.W., 1999. Measurement of mitochondrial membrane potential using fluorescent rhodamine derivatives. Biophys. J. 76, 469–477.
Schep, L.J., Slaughter, R.J., Vale, A., Beasley, M., Gee, G.P., 2011. The clinical toxicology of the designer "party pills" benzylpiperazine and trifluoromethylphenylpiperazine. Clin. Toxicol. 49, 131–141.
Smith, J.A., Weidemann, M.J., 1993. Further characterization of theneutrophil oxidative burst by flow cytometry. J. Immunol. Methods 162, 261–268.
Staack, R.F., Fritschi, G., Maurer, H.H., 2003. New designer drug 1-(3-trifluoromethylphenyl)piperazine (TFMPP): gas chromatography/mass spectrometry and liquid chromatography/mass spectrometry studies on its phase I and II metabolism and on its toxicological detection in rat urine. J. Mass Spectrom. 38, 971–981.
Staack, R.F., Maurer, H.H., 2004. New designer drug 1-(3,4-methylenedioxybenzyl) piperazine (MDBP): studies on its metabolism and toxicological detection in rat urine using gas chromatography/mass spectrometry. J. Mass Spectrom. 39, 255–261.
Staack, R.F., Maurer, H.H., 2005. Metabolism of designer drugs of abuse. Curr. Drug Metab. 6, 259–274.
Staack, R.F., Paul, L.D., Schmid, D., Roider, G., Rolf, B., 2007. Proof of 1-(3-chlorophenyl)piperazine (mCPP) intake – use as adulterant of cocaine resulting in drug–drug interations? J. Chromatogr. B 855, 127–133.
Staack, R.F., Theobald, D.S., Paul, L.D., Springer, D., Kraemer, T., Maurer, H.H., 2004. In vivo metabolism of the new designer drug 1-(4-methoxyphenyl)piperazine (MeOPP) in rat and identification of the human cytochrome P450 enzymes responsible for the major metabolic step. Xenobiotica 34, 179–192.
Thompson, I., Williams, G., Caldwell, B., Aldington, S., Dickson, S., Lucas, N., McDowall, J., Weatherall, M., Robinson, G., Beasley, R., 2010. Randomised double-blind, placebo-controlled trial of the effects of the 'party pills' BZP/TFMPP alone and in combination with alcohol. Psychopharmacology (Berl.) 24, 1208–1299.
Tiangco, D.A., Lattanzio Jr, F.A., Osgood, C.J., Beebe, S.J., Kerry, J.A., Hargrave, B.Y., 2005. 3,4-Methylenedioxymethamphetamine activates nuclear factor-κB, increases intracellular calcium, and modulates gene transcription in rat heart cells. Cardiovasc. Toxicol. 5, 301–310.
Watkins, S.J., Borthwick, G.M., Arthur, H.M., 2011. The H9C2 cell line and primary neonatal cardiomyocyte cells show similar hypertrophic responses in vitro. In Vitro Cell. Dev. Biol. Anim. 47, 125–131.
Weyermann, J., Lochmann, D., Zimmer, A., 2005. A practical note on the use of cytotoxicity assays. Int. J. Pharm. 288, 369–376.
Wood, D.M., Button, J., Lidder, S., Ramsey, J., Holt, D.W., Dargan, P.I., 2008. Dissociative and sympathomimetic toxicity associated with recreational use of 1-(3-trifluoromethylphenyl)piperazine (TFMPP) and 1-benzylpiperazine (BZP). J. Med. Toxicol. 4, 254–257.
Yarana, C., Sripetchwandee, J., Sanit, J., Chattipakorn, S., Chattipakorn, N., 2012. Calcium-induced cardiac mitochondrial dysfunction is predominantly mediated by cyclosporine A-dependent mitochondrial permeability transition pore. Arch. Med. Res. 43, 333–338.
Yuan, C., Acosta Jr, D., 1996. Cocaine-induced mitochondrial dysfunction in primary culture of rat cardiomyocytes. Toxicology 112, 1–10.
Zhang, H., Forman, H.J., Choi, J., 2005. Gamma-glutamyl transpeptidase in glutathione biosynthesis. Methods Enzymol. 401, 468–483.
Zordoky, B.N.M., El-Kadi, A.O.S., 2007. H9c2 cell line is a valuable in vitro model to study the drug metabolizing enzymes in the heart. J. Pharmacol. Toxicol. Methods 56, 317–322.
Zwolak, I., 2013. Comparison of five different *in vitro* assays for assessment of sodium metavanadate cytotoxicity in Chinese hamster ovary cells (CHO-KI line). Toxicol. Ind. Health 1–14 doi:http://dx.doi.org/10.1177/0748233713483199.